Quaternary Research 72 (2009) 1–15

Contents lists available at ScienceDirect

Quaternary Research

journal homepage: www.elsevier.com/locate/yqres

Stratigraphy, depositional environments and level reconstruction of the last interglacial Lake Samra in the Dead Sea basin

N. Waldmann [a,*], M. Stein [b], D. Ariztegui [c], A. Starinsky [a]

[a] The Institute of Earth Sciences, The Hebrew University of Jerusalem, Givat Ram, 91904-Jerusalem, Israel
[b] The Geological Survey of Israel, 30 Malkhei Yisrael St., 95501-Jerusalem, Israel
[c] Earth Sciences Section, University of Geneva, Rue des Maraichers 13, 1205-Geneva, Switzerland

ARTICLE INFO

Article history:
Received 28 August 2007
Available online 21 May 2009

Keywords:
Last interglacial
Dead Sea basin
Lacustrine depositional environments
Paleoclimate
Paleolimnology
Sequence stratigraphy
Lake level
Sedimentary basins

ABSTRACT

In this paper we describe the stratigraphy and sediments deposited in Lake Samra that occupied the Dead Sea basin between ~135 and 75 ka. This information is combined with U/Th dating of primary aragonites in order to estimate a relative lake-level curve that serves as a regional paleohydrological monitor. The lake stood at an elevation of ~340 m below mean sea level (MSL) during most of the last interglacial. This level is relatively higher than the average Holocene Dead Sea (~400 ± 30 m below MSL). At ~120 and ~85 ka, Lake Samra rose to ~320 m below MSL while it dropped to levels lower than ~380 m below MSL at ~135 and ~75 ka, reflecting arid conditions in the drainage area. Lowstands are correlated with warm intervals in the Northern Hemisphere, while minor lake rises are probably related to cold episodes during MIS 5b and MIS 5d. Similar climate relationships are documented for the last glacial highstand Lake Lisan and the lowstand Holocene Dead Sea. Yet, the dominance of detrital calcites and precipitation of travertines in the Dead Sea basin during the last interglacial interval suggest intense pluvial conditions and possible contribution of southern sources of wetness to the region.

© 2009 University of Washington. Published by Elsevier Inc. All rights reserved.

Introduction

During the Quaternary several lakes have occupied the tectonic depressions along the Dead Sea transform (DST): the mid- to late Pleistocene Lake Amora, the last interglacial Lake Samra, the last glacial Lake Lisan and the Holocene to modern Dead Sea (Neev and Emery, 1967; Stein, 2001; Bookman et al., 2006; Torfstein, 2008). The limnological conditions of these lakes (e.g., levels, structure and chemistry) were largely affected by hydrological changes in their watershed (Stein, 2001; Enzel et al., 2003). Their sedimentary record, therefore, serves as regional paleoclimatological gauges that consistently recorded wet and dry episodes at all temporal scales.

This study focuses on the sedimentological and limnological history of Lake Samra that occupied the Dead Sea basin (DSB) during the last interglacial. Well-exposed stratigraphic sections from onshore to lake-margin and deeper lacustrine environments are available for reconstruction of the paleoenvironmental conditions and stratigraphy architecture (following similar works such as Manspeizer, 1985, and Bartov et al., 2007, among others). The remarkable preservation of lacustrine and fluvial archives from the last interglacial Dead Sea area provides insights into the paleoclimatological conditions of this region, which are still mostly unknown for this period of time. In this work we present the first systematic documentation of sedimentary sections of the Samra Formation (that was deposited from Lake Samra) and the reconstruction of its depositional environments. Combining the sedimentological and stratigraphic information with U-series dating of primary aragonites, we were able to estimate the lake-level history for the time interval between ~130 and 75 ka. The reconstructed lake level is compared to other records in order to understand potential regional and global climatic forcing during the last interglacial.

Regional geology and previous studies

The DSB is the deepest continental pull-apart basin formed along the DST (Garfunkel, 1981; Ben-Avraham, 1997). During the Miocene, the basin was filled by fluvio-lacustrine deposits of the Hazeva Formation (Garfunkel, 1981). Later during the Pliocene, the Mediterranean Sea intruded the DSB forming the Sedom lagoon that deposited thick sequences of salts (Zak, 1967). After the disconnection of the lagoon from the open sea, terminal lacustrine bodies successively occupied the basin: the middle to late Pleistocene Lake Amora, the last interglacial Lake Samra (the subject of this paper), the last glacial Lake Lisan, and the Holocene Dead Sea (e.g., Stein, 2001; Bookman et al., 2006) (Fig. 1).

* Corresponding author. Department of Earth Science, University of Bergen, Allégaten 41, 5007-Bergen, Norway.
E-mail address: nicolas.waldmann@geo.uib.no (N. Waldmann).

0033-5894/$ – see front matter © 2009 University of Washington. Published by Elsevier Inc. All rights reserved.
doi:10.1016/j.yqres.2009.03.005

https://doi.org/10.1016/j.yqres.2009.03.005 Published online by Cambridge University Press

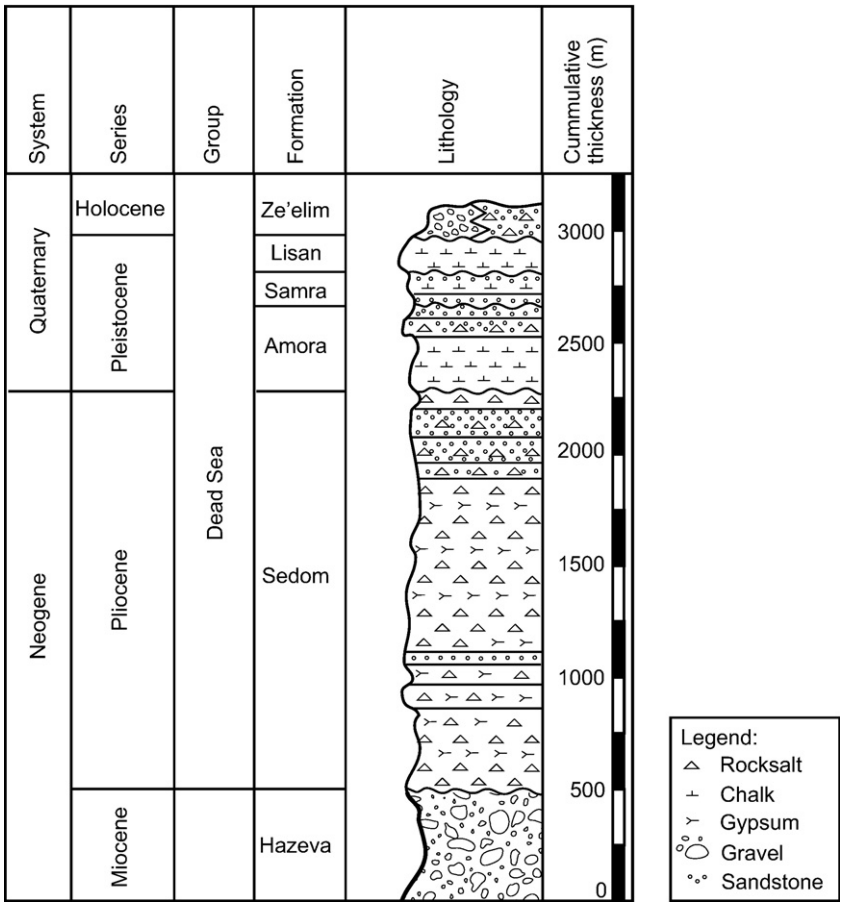

Figure 1. General stratigraphic section of the Dead Sea Group (adapted from Zak, 1967).

Whereas the last glacial Lake Lisan and the Holocene Dead Sea have been widely studied during the past few decades, providing significant archives of paleoenvironmental changes (e.g., Neev and Emery, 1967; Begin et al., 1974; Katz et al., 1977; Stein et al., 1997; Enzel et al., 2006), little is known about their last interglacial predecessor, Lake Samra. The sediments deposited from this lake and its surroundings (composing the Samra Formation) are exposed along the DSB from the Iddan region in the south to the central Jordan Valley in the north (Fig. 2). The formation was first described in the Jericho area north of the Dead Sea as fluvio-lacustrine deposits (Picard, 1943; Rot, 1969; Begin et al., 1974; Begin, 1975). Zak (1967) correlated these exposures with the upper part of the Amora Formation, which were mapped around the Mt. Sedom salt diapir, south of the Dead Sea. Other sedimentary units from the DSB were associated with the Samra Formation (e.g., Bentor and Vroman, 1960; Langozky, 1961; Sneh, 1982; Manspeizer, 1985; Kaufman et al., 1992; Weinberger et al., 2000); however, a complete sedimentary description of these deposits was lacking as well as their spatial correlation.

Environments of deposition

The sediments deposited in Lake Samra and its surroundings (the Samra Formation) represent several depositional environments similar to those previously described in detail for Lake Lisan and the Holocene Dead Sea (Machlus et al., 2000; Bartov et al., 2002; Bookman (Ken-Tor) et al., 2004 and references therein). The following sedimentary environments are discussed in this paper: 1) the onshore depositional environment, which includes alluvial and fluvial deposits; 2) the marginal lacustrine environment, which consists of a relatively narrow zone at andvalong the shore; and 3) the offshore lacustrine environment that includes deposits from different water depths. Specific lithofacies were recognized in these depositional environments based on systematic differences in grain size, sedimentary structures and textures, amount of clastic material, and bedding characteristics.

Onshore environments include mainly stream fan deltas, and alluvial and fluvial plains. At the lake margins, breaking waves wash away finer sediments building beach ridges that consist of pebbles or coarse sand (Bartov et al., 2007). In flat areas such as the southern extreme of the basin, however, oolites cover extensive areas (Sneh, 1982), occasionally interfingering with travertines (Enmar, 1999; Waldmann 2002; Waldmann et al., 2007). As deposits are shifted toward deep water, the influence of waves on deposition is reduced and grain size diminishes. The sediments may exhibit ripple marks, flute structures and cross-bedding as a consequence of wave energy variations. Clay- to silt-size laminated deposition takes place in the lacustrine environment indicating periods of layered-lake configuration, similar to that in Lake Lisan (Stein et al., 1997). It should be highlighted, however, that while primary aragonite (deposited from the lake water) is a major constituent of the Lisan Formation, it seldom appears in the offshore lacustrine sedimentary sequences of the Samra Formation, which consists mainly of calcitic marls (Waldmann et al., 2007).

Sequence stratigraphy

The lithofacies associations described above, recognized in the different stratigraphic successions, represent regressive and trans-

https://doi.org/10.1016/j.yqres.2009.03.005 Published online by Cambridge University Press

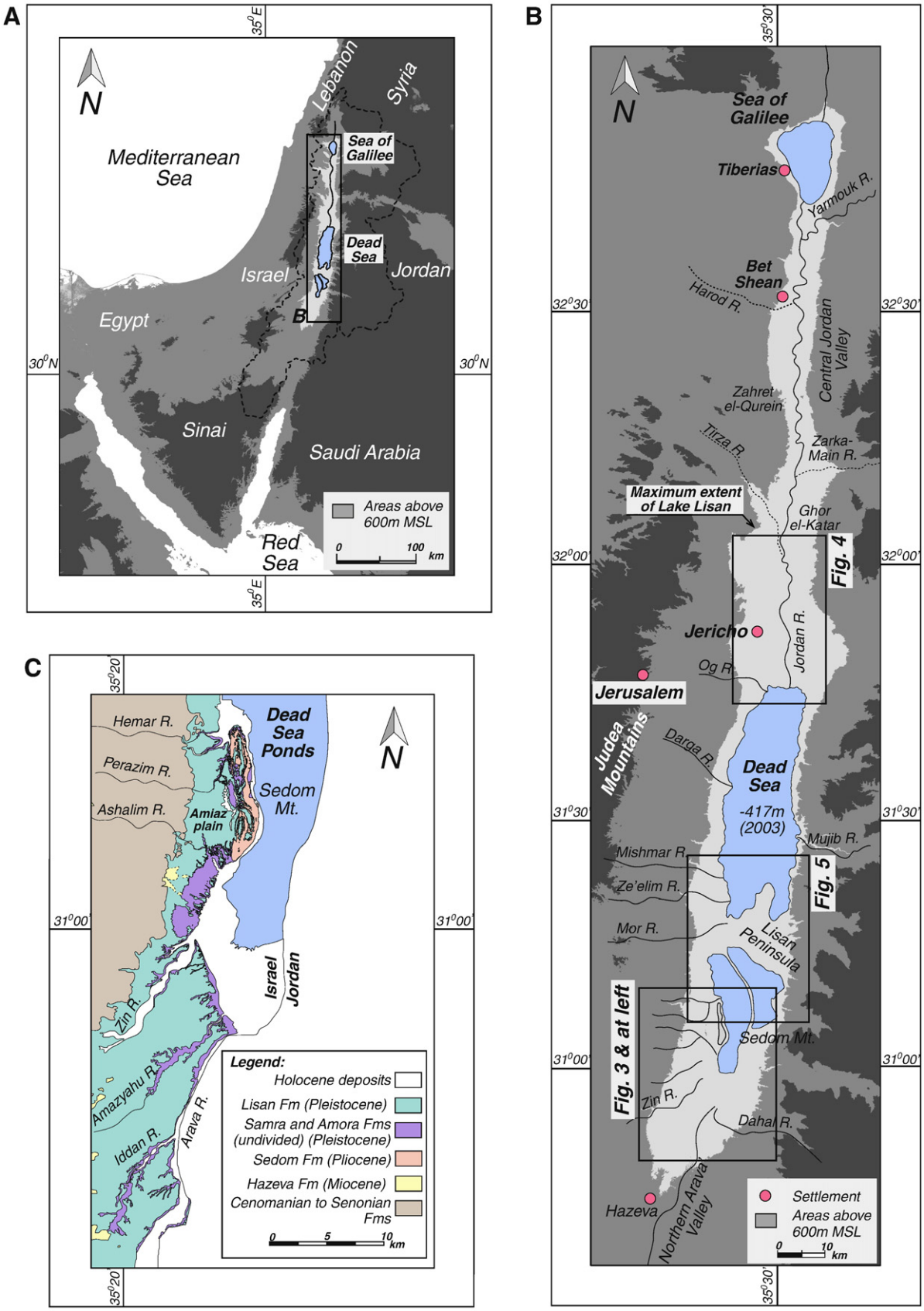

Figure 2. (A) Map of the Levant highlighting the Dead Sea and Jordan Valley. Dashed line outlines the Dead Sea watershed. (B) The Dead Sea, Jordan Valley, and Sea of Gelilee regions. The maximum extent of Lake Lisan during the LGM is shown in light gray. (C) Geologic map of the southern Dead Sea area showing main divisions of the Quaternary and pre-Quaternary DSB deposits (modified from Zak 1967; Waldmann, 2002).

https://doi.org/10.1016/j.yqres.2009.03.005 Published online by Cambridge University Press

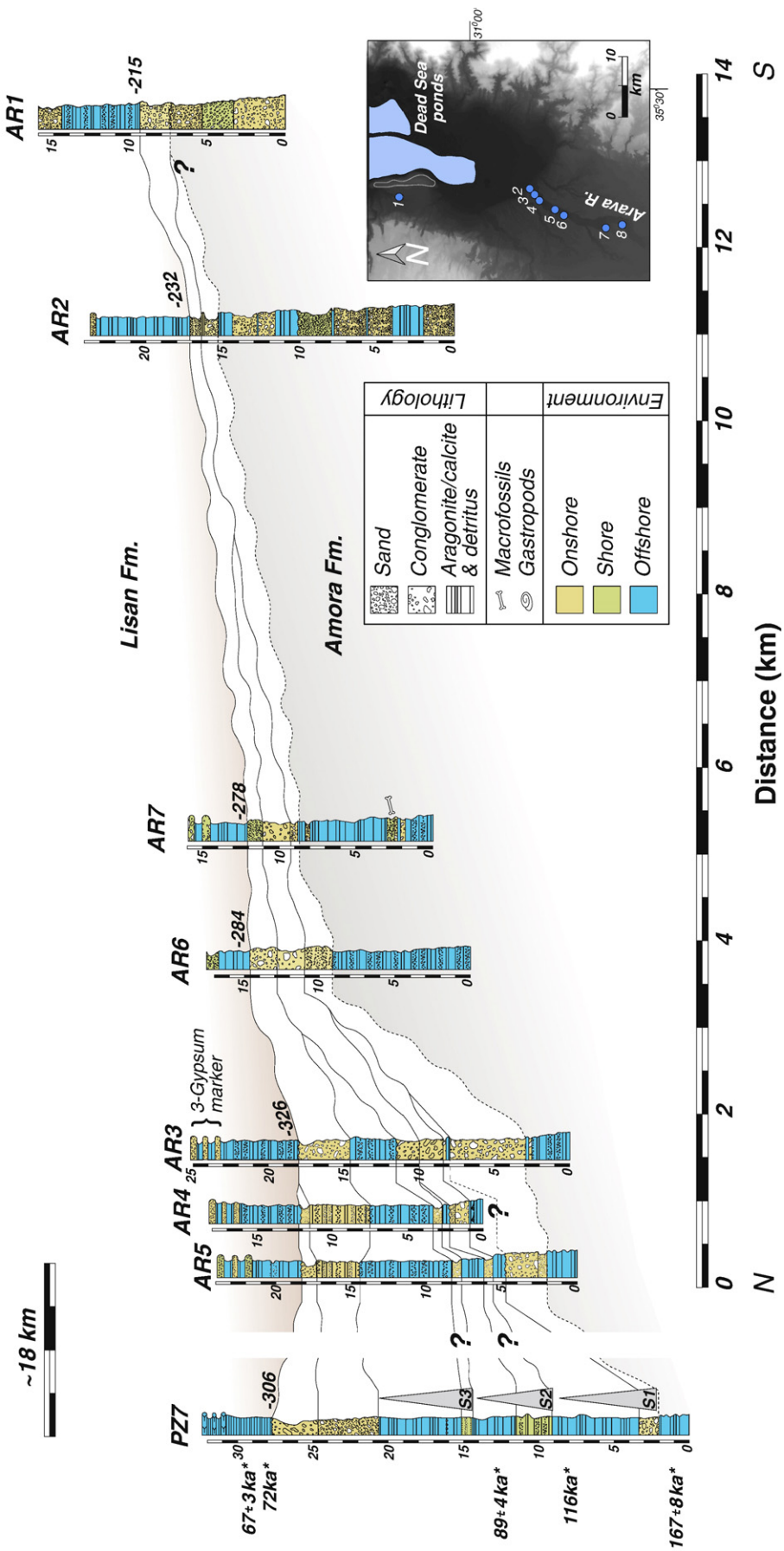

Figure 3. Stratigraphic correlation between outcrops in the southernmost extreme of the DSB. Locations of sites are shown on the Digital Elevation Model (DEM) map: 1) Perazim 7 columnar section (PZ7), 2 to 8) Arava columnar sections (AR5, AR4, AR3, AR6, AR7, AR2 and AR1, correspondingly). U/Th ages at the PZ7 columnar section from Waldmann et al. (2007). Three sequences are recognized within the Samra record: S1 to S3, which are related to lake levels as shown in Figures 6 and 7. Note the increased distance between the PZ7 columnar section and the AR columnar sections, which makes this correlation of ages and sequences a proposed correlation. Height of the different columnar section is in m below mean sea level and measured at the transition between the Samra and Lisan formations.

https://doi.org/10.1016/j.yqres.2009.03.005 Published online by Cambridge University Press

gressive episodes of the lake. The sequence architecture of the Samra sediments is, therefore, attributed to three factors: lake-level fluctuations, initial topography/morphology and availability of detrital material (following Posamentier et al., 1992). In flat areas surrounding the basin, correlations among stratigraphic sections include intercalations of onshore and offshore deposits allowing reconstruction of the lake-level behavior. Taking into consideration the large size of the DSB and distances among the different outcrops, we documented separately the stratigraphy of the Samra Formation in the southern, northern, and central parts of the basin.

The southern DSB

The stratigraphy of the southern extreme of the DSB is based on seven measured sections covering a distance of over 14 km along the western side of the Arava valley (Fig. 3). The correlation between the Arava sections is based on marker beds that were physically traced in the field and later compared to the same horizons dated in the Perazim 7 (PZ7) columnar section (Appendix A, on-line supplemental material). We emphasize, however, that this correlation is one possible interpretation under the existing limited age information. Distances between the columnar sections were measured using an electronic distance measurement (EDM) and elevations confirmed with differential GPS. The chronological framework is based on several U/Th ages (Waldmann et al., 2007) that were obtained from aragonite laminae in the PZ7 columnar section and are summarized in Table 1.

Five main sequences defined by major unconformities were identified in the exposures. The uppermost sequence stands for the Lisan deposits, which was recognized by internal lithological markers such as thick packages of purely laminated aragonite and detritus and defined gypsum beds (Bartov et al., 2002; Torfstein et al., 2008). The lowermost sequence is identified as part of the Amora Formation based on the correlation of the sections in the northernmost Arava valley with the PZ7 columnar section. Both these lowermost and uppermost sequences were not considered in the stratigraphic analysis, while we focus here only on sequences S1 to S3 (Fig. 3).

The S1 sequence partially outcrops in the Arava valley in sections AR5, AR4 and AR3 consisting of pebble and cobble layers fining-upward to intercalations of silt and clay. Both the base and top of this unit are confined by erosional unconformities. The entire sequence thickens northwards with the increment of larger clast grain sizes in those areas in relation to fluvial input. Thus, the elevation of the sequence represents the highest possible lake level during this period of deposition. An estimation of the S1 age is derived by correlation with the PZ7 columnar section (considering possible caveats due to the large distance), where an age of approximately 116 ka was obtained at ~5 m above the sequence's base (Table 1).

Sequence S2 is exposed at the northernmost sections of the Arava valley as well and is characterized by a fining-upward succession bounded by erosional surfaces. The sequence begins with coarse well-rounded clastic sediments overlain by intercalations of marls and fine silts, probably indicating a lake-level drop that was followed by a minor lake-level rise. As in S1, the age of S2 was estimated by correlation to PZ7, where a U/Th age of ~89 ka was obtained from the laminated section 4 m above the sequence base (Table 1). Identifying no major unconformities and hiatuses within the lacustrine part of the sequence, we estimate that S2 was deposited between ~115 and ~85 ka.

The overlying S3 sequence is similar to the previous sequences consisting of a fining-upward succession that starts with coarse and rounded clastic sediments overlain by intercalations of marls and fine silts. It reaches a maximum thickness at the northern AR5 columnar section while thinning and completely being eroded southwards. Overall, this sequence shows a transition from alluvial and fluvial deposits in the southernmost sites to a lake setting in the north. Although there is no dated material in this sequence, we estimate its age by constraining the top of this cycle with a U/Th age obtained ~1 m above the basis of the Lisan Formation in the PZ7 columnar section. The retrieved U/Th age yielded ~67 ka, thus placing this sequence between ~85 and 75–70 ka. S3 is interpreted as representing a short-term lake-level rise in the basin.

The northern DSB

A stratigraphical correlation was physically traced in the northern DSB among four measured sections located along the western flanks of the Jordan River and following the basin axis (Fig. 4). Overall, the laminated lacustrine-type deposits thicken southward as the clastic material increase northward, probably related to increase clastic input by the Jordan and Tirza rivers (Fig. 2 for location). The stratigraphic boundary between the Samra and Lisan formations was identified by distinctive markers within the Lisan Formation (e.g., the triple gypsum unit; Bartov et al., 2002) and is chronologically constrained by U/Th ages retrieved at the Bet Ha'Arava columnar section (BA). At this locality, an age of 72 ± 3 ka was retrieved 20 cm above this transition while an age of 108 ± 12 ka was recovered ~1 m below it indicating a prominent depositional hiatus (Fig. 4, Table 1 and Appendix B, on-line supplemental material). North of the Bet Ha'Arava columnar section, the transition between the Samra and Lisan formations is characterized by a 1.5-m-thick paleosol horizon enriched with gastropods, suggesting local increase in wetness.

The central DSB

Three columnar sections were erected in the central sector of the western Dead Sea margin: Massada (MZ), Mishmar (MS) and Mor (MR) (Appendixes C, D and E, respectively in the on-line supplemental material). The different sites are further correlated to the previously described PZ7 columnar section (Fig. 5). Since no physical continuation exists between these outcrops, the stratigraphic correlation was not performed in a typical "onshore to

Table 1
U/Th ages of Samra and Lisan aragonites (modified from Waldmann et al., 2007).

Sample	DSB location	Location	Elevation m MSL (a)	Elevation A/B transition (b)	Age ka	Error	Source (c)
PZ1-L6	South	Perazim	−305	1	67.4	3.4	1
n.a.		Perazim	−322	−16	116	n.a.	2
PZ2-7		Perazim	−328	−22	167.2	8.4	1
MZ-2	Central	Massada	−372	2	68.1	3.4	1
MZ-5		Massada	−375	−1	75.6	3.8	1
MZ-7		Massada	−380	−6	90.4	4.5	1
MR-23		Mor	−385	−1	71.5	3.6	1
MR-6		Mor	−386	−2	76.8	6.1	1
MS-4		Mishmar	−374.8	0.2	75.3	3.8	1
MS-7		Mishmar	−375	0.05	80.2	4.0	1
MS-1		Mishmar	−375	−0.1	87.1	4.4	1
MS-10		Mishmar	−375.5	−0.5	88.9	4.4	1
BA-3	North	Beit-Ha'Arava	−364.8	0.2	71.6	3.0	1
BA-5		Beit-Ha'Arava	−365.6	−0.6	107.9	12.6	1

For site location see Figures 5, 6 and 7 (northern, southern and central sites, correspondingly). Comments: a) sample elevation in meters below mean sea level; b) sample elevation in relation to the stratigraphical transition between the Samra and Lisan formations; c) sources: 1: Waldmann et al. (2007); 2: Kaufman et al. (1992).

https://doi.org/10.1016/j.yqres.2009.03.005 Published online by Cambridge University Press

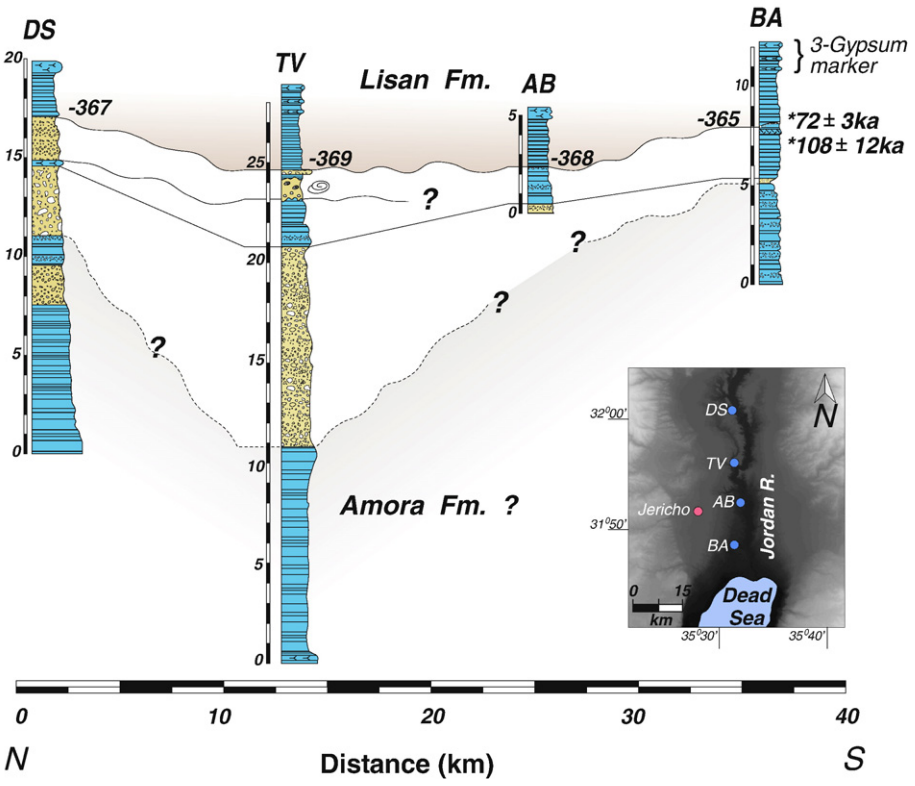

Figure 4. Suggested stratigraphic correlation between outcrops in the northernmost part of the DSB. Locations of sites are shown on the DEM map: DS: Deir Shaman, TV: Tovlan, AB: Allenby bridge and BA: Bet Ha'Arava. U/Th ages at the BA columnar section from Waldmann et al. (2007) and are resumed in Table 1. DS and AB columnar sections modified from Begin et al. 1974. Heights of the different columnar sections are in m below mean sea level measured at the transition between the Samra and Lisan formations. See Figure 3 for legend.

offshore" pattern (e.g., the proposed correlations in Figs. 3 and 4) but rather parallel to the lake's western shore. To minimize truncation by streams entering the basin from the west, the different sites were chosen in the terraces at the sides of present-day (and late Pleistocene) fan deltas, thus reducing possible traces of erosion.

The three sites are mainly dominated by alternation of laminated lacustrine deposits, which are occasionally interrupted by sand and gavel layers interpreted as beach sediments. The information gathered from the elevations and ages of those shore deposits is crucial in reconstructing the lake-level variations. The stratigraphic boundaries between internal sub-units were constrained by several U/Th ages and recognition of distinct lithological markers (e.g., the triple gypsum unit; Bartov et al., 2002).

Chronology and level reconstruction of Lake Samra

The lake-level history proposed here (Fig. 6) is based on a combination of direct level indicators constrained chronologically in the southern, northern and central regions, as described in the previous section. The current effort to reconstruct the level curve for Lake Samra follows similar studies by Bartov et al. (2002; 2007) on Lake Lisan and Bookman (Ken-Tor) et al. (2004) and Bookman et al. (2006) on the Holocene Dead Sea. However, we are aware that in the case of the Samra Formation that both the exposures and the suitable material (primary aragonite) for U/Th age control are limited. Nevertheless, the above described dataset allow for some suggestions and several important conclusions regarding the paleoenvironmental setting of the DSB during the last interglacial interval. The dated samples considered for the lake-level reconstruction come from primary aragonite laminae that closely bound shallow-water indicator sediments such as beach deposits. In addition, we assume a minimal deposition rate of about 1 mm/yr in the lacustrine deposits, which is slightly higher then the rate estimated for the laminated lacustrine sediments (primary aragonite and silty detritus) comprising the Lisan Formation (ca. 0.8 mm/yr; Schramm et al., 2000). Low lake levels are estimated from the lowest elevation where the sequence boundary exhibits erosional features, while high levels are estimated from the highest elevation of lacustrine units in the sequence (Fig. 6). This technique overestimates the absolute lake-level heights, providing a pattern of regressions and transgressions and potential relative changes in lake level.

The transition between the Amora and Samra formations is defined at the base of the S1 sequence (Fig. 6). This proposition is based on a U/Th age of ~167 ± 4 ka measured on aragonite lamina approximately one meter below the S1 sequence in the PZ7 columnar section. Aragonite laminae of similar glacial Marine Isotope Stage (MIS) 6 ages compose the upper Amora Formation described on the eastern side of Mt. Sedom (Torfstein, 2008). Considering the U/Th age of ~116 ka retrieved from aragonite laminae within the S1 sequence and the proposed sedimentation rate, we suggest that the transition between the Amora and Samra formations is located ~130–140 ka, which is consistent with the transition between MIS 6 and 5 in the global records. Taking into consideration a tectonic subsidence of 0.3 mm/yr for western margins of the DSB (Bartov et al., 2006), the onshore deposits that dominate the lower part of the S1 sequence (Figs. 3, 4 and 5) were deposited during a lake stand lower than ~380 m below mean sea level (MSL) (Fig. 6). Following this lowstand, the lake level rose to elevations higher than ~320 m below MSL at ~120 ka depositing relatively thick units of laminated lacustrine sediments (>5 m in the PZ7 columnar section; Appendix A in the

https://doi.org/10.1016/j.yqres.2009.03.005 Published online by Cambridge University Press

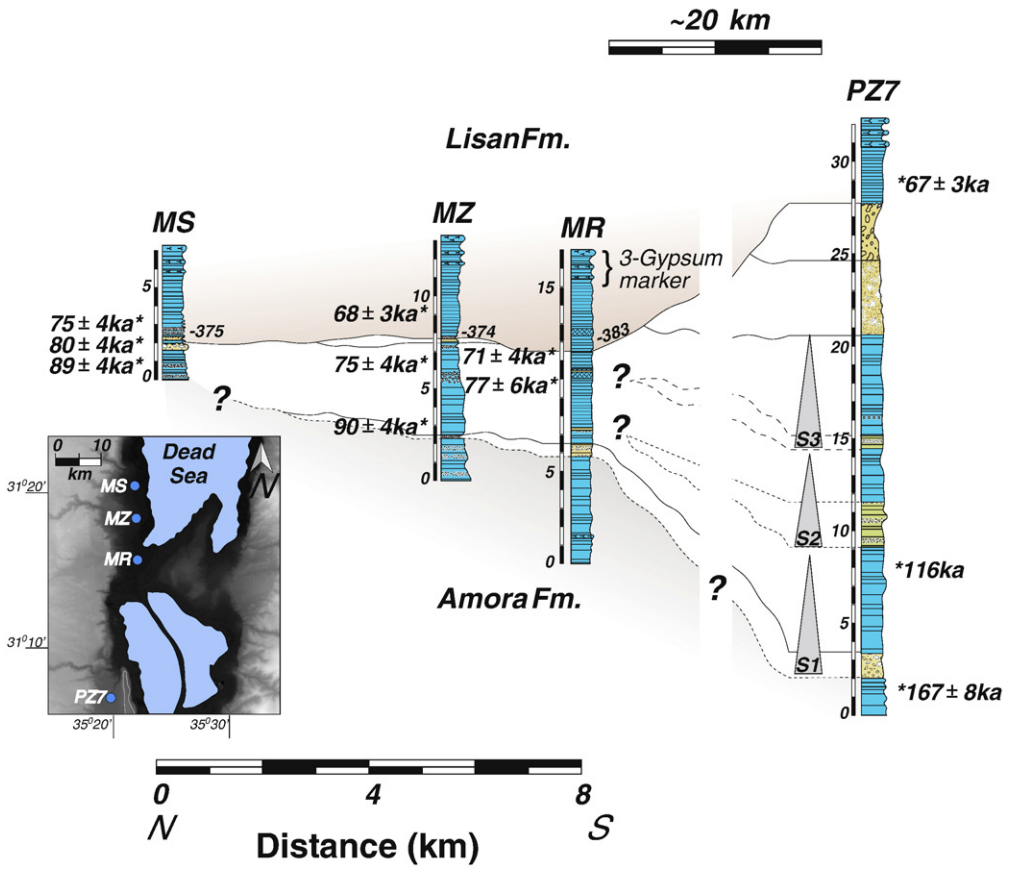

Figure 5. Proposed chronostratigraphic correlation between outcrops in the central part of the DSB compared to the PZ7 columnar section. Locations of sites are shown on the DEM map: MS: Mishmar, MZ: Massada, MR: Mor and PZ7: Perazim 7. U/Th ages from Waldmann (2002) and Waldmann et al. (2007) and are resumed in Table 1. Heights of the different columnar sections are in m below mean sea level measured at the transition between the Samra and Lisan formations. Note the enlarged distance between the central sites to the PZ7 columnar section. See legend in Figure 3.

on-line supplemental material). This elevation is estimated by correlating the exposures in the Arava valley (Fig. 3) and considering a lower subsidence rate in that region (~0.2 mm/yr) (Ben-Avraham and Schubert, 2006). Subsequently, the lake level dropped again to ~340–350 m below MSL at an estimated age of 116 ka (as extrapolated from the chronology obtained in the central region and exposure of shore deposits in the southern region; Figs. 5 and 3, respectively). During the S2 sequence the lake rose again above ~310–320 m below MSL (Fig. 6), considering elevations and ages of erosional surfaces recognized at the Arava valley (Fig. 3). Approximately 90 ka, the lake receded again and fluctuated several times during sequence S3 before the rise of Lake Lisan at ~75 ka to 260 m below MSL (Fig. 6) (Bartov et al., 2002; Waldmann et al., 2007). The upper boundary of the Samra Formation is placed at the sequence S3 termination (~80–75 ka) marking the transition to the last glacial Lisan Formation (MIS 4 to 2). Thus, the suggested chronology and distinctive lithology identifies the Samra Formation as an independent chronostratigraphical unit composing sedimentary sequences that were deposited during the last interglacial period.

In summary, the lithology and chronology of the described exposures of the Samra Formation suggest that the lake fluctuated mostly between ~310 and ~350 m below MSL. The estimated Lake Samra levels are ~50–100 m higher than the mean level of the Holocene Dead Sea (Bookman (Ken-Tor) et al., 2004; Bookman et al., 2006; Migowski et al., 2006). This hydrological difference may indicate a relative wetter regime during the last interglacial compared to present conditions, or else changes in the tectonic subsidence rate of the basin.

Paleohydrological and paleoclimatic implications

The transition between lakes Samra and Lisan was accompanied by a distinct lithological-geochemical change: Lake Samra deposited mainly detrital calcites and some primary calcite while Lake Lisan precipitated mainly primary aragonite, silty detritus and gypsum. Waldmann et al. (2007) proposed that the limited amount of aragonite precipitating during the Samra period reflects diminishing contribution of the Dead Sea Ca-chloride brines to the lake. This, in turn was related to lower amounts of rain above the Judea Mountains during the last interglacial period. Moreover, the deposition of laminated calcites in the Samra Formation indicates fresher water conditions compared to Lake Lisan.

Lake Samra was fed by sporadic freshwater floods loaded with substantial amounts of detrital calcites; however, the transport of bicarbonate required for aragonite production was limited (Waldmann et al., 2007). The paleohydrological and paleoclimatic implications that are derived from the lithological assemblages of both the Samra and Lisan formations are corroborated by the lake-level patterns. Lake Lisan levels were substantially higher than those of Lake Samra (Fig. 7b). The differences in levels and lithology (Lisan: primary aragonite and gypsum; Samra: detrital calcites) indicate that the drainage area of the DSB was overall more arid during the last interglacial (Samra) interval than during the glacial (Lisan) period. Moreover, the last interglacial was characterized by sporadic floods, while the glacial interval was distinguished by regular supply of water.

Following paleoclimatic interpretations from the global sea-level curve deduced from coral records (Fig. 7e) (e.g., Stein et al., 1993;

https://doi.org/10.1016/j.yqres.2009.03.005 Published online by Cambridge University Press

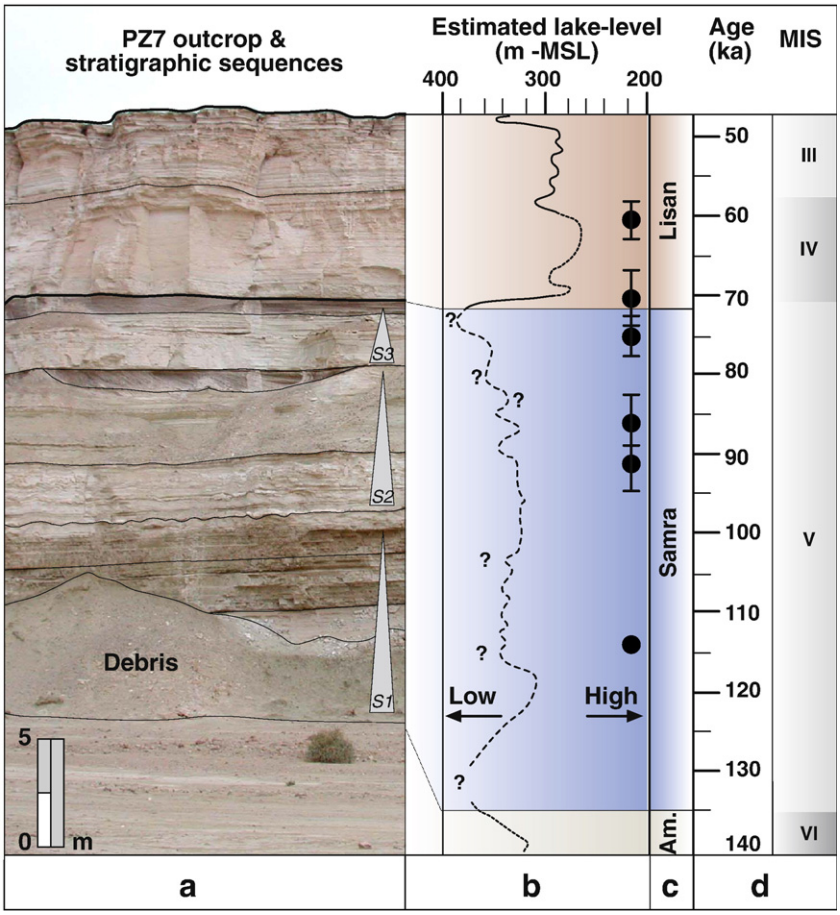

Figure 6. The reconstructed Samra lake-level curve. a) A photograph of the PZ7 columnar section with the local stratigraphic cycles. b) The lake-level curve between ~140 and 50 ka. Black dots mark heights of absolute dating by U/Th. The Lisan lake-level curve is adapted from Bartov et al. (2003). Samra lake levels are estimated and represent maximum or minimum heights. c) Stratigraphy of the DSB lacustrine deposits. Am. stands for Amora. d) Timing of Marine Isotope Stages (following EPICA community members, 2006).

Cutler et al., 2003; Hearty et al., 2007), a significant deglaciation occurred at ~135 ka, which is the estimated time of transition between lakes Amora and Samra. The lake dropped significantly around that time (probably below 380 m below MSL, Fig. 7b) resembling the drop of Lake Lisan during termination I (Stein and Goldstein, 2006). It is thus implied that the terminations and major sea-level rises are accompanied by major aridity in the Levant region. The terminations are also reflected by negative shifts in the oxygen isotope values of Mediterranean foraminifers (Fontugne and Calvert, 1992) (Fig. 7d) as well as cave speleothems in central and southern Israel (Bar-Matthews et al., 2003; Vaks et al., 2006) (Fig. 7c). Kolodny et al. (2005) interpreted the $\delta^{18}O$ shifts of both cave speleothems and Lisan aragonites as mainly reflecting the source composition in the east Mediterranean seawater, which in turn control the Levant meteoric precipitation.

Since the chronology and level reconstruction of Lake Samra are of relatively low resolution, it is not possible to properly correlate short episodes of level change in both the ocean and lake records. It seems that the ~105 ka sea-level rise, however, is also reflected by a lowstand in the lake, while the cold episodes in the Northern Hemisphere at ~110, 95 and 85 ka (Cutler et al., 2003) could be correlated with minor rises of Lake Samra. A similar behavior is portrayed by Lake Lisan and the Holocene Dead Sea when the lake levels are higher during the cold glacial interval and lower during the warm interglacial (or interstadials) (Bartov et al., 2002; 2003; Bookman (Ken-Tor) et al., 2004). This correspondence calls for a very close relation between global climate, as reflected by global sea-level changes (mainly responding to ice formation or melting), and the Levant regional hydrology. The glacial periods, and even short stadials, are wetter in the Levant, while the interglacial periods, and particularly the terminations, are arid leading to significant lake-level fall. Nevertheless, the dominance of detrital calcites in the sedimentary sequences deposited in Lake Samra during the last interglacial calls for intensive floods and sediment transport to the basin. Speleothems in the Negev desert (Vaks et al., 2006) and travertines in the Arava valley (Enmar, 1999; Waldmann et al., 2007) record similar pluvial conditions during the same time interval. These findings may imply increase regional humid conditions, probably in relation to a southern source during the last interglacial.

Conclusions

1) Lake Samra occupied the tectonic depression of the Dead Sea basin during the last interglacial between ~135 and 75 ka. Its levels fluctuated mostly around 340 ± 20 m below MSL, significantly lower than the last glacial Lake Lisan (mostly between 280 ± 20 m below MSL) but higher than the Holocene Dead Sea (mostly 400 ± 30 m below MSL). Considering the levels of these terminal lakes as regional paleohydrological monitors, the Samra period was overall drier than the Lisan but wetter than the Holocene.
2) Based on facies associations and stratigraphic successions the Samra Formation is divided into three sequences (S1 to S3). S1 was

https://doi.org/10.1016/j.yqres.2009.03.005 Published online by Cambridge University Press

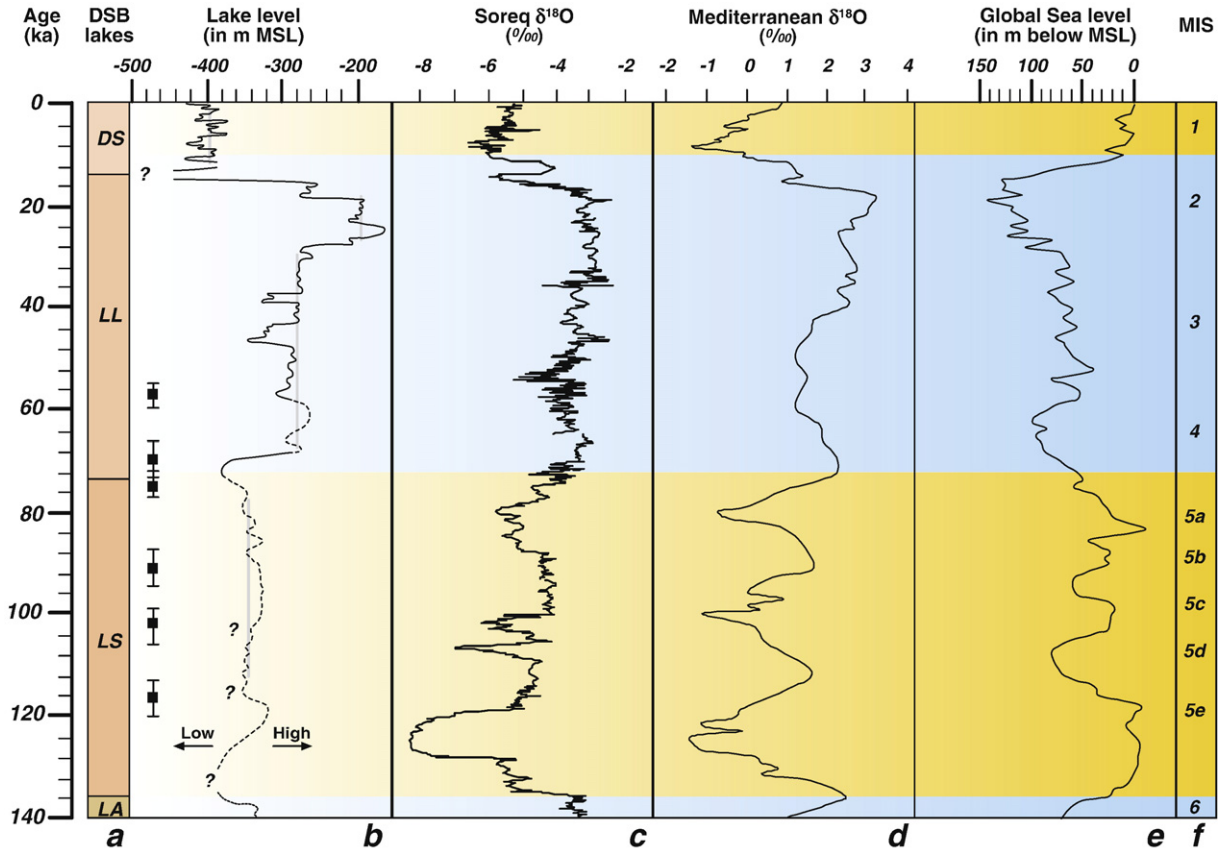

Figure 7. Comparison of lake levels in the DSB with global climatic events. a) Timing of the different evolving lakes in the DSB, DS: Dead Sea, LL: Lake Lisan, LS: Lake Samra and LA: Lake Amora. b) The entire reconstructed DSB lake-level curve for the last 140 ka. The Lisan and Dead Sea lake-level curves are taken from Bartov et al. (2003) and Bookman (Ken-Tor) et al. (2004), respectively. Grey line marks average elevation of the different water bodies. Small black squares stand for absolute U/Th dating shown in this work. c) Variations of $\delta^{18}O$ values from Soreq speleothems (Bar-Matthews et al., 2003). d) East Mediterranean $\delta^{18}O$ record from foraminifera *G. rubber* (Fontugne and Calvert, 1992). e) The global sea-level curve (after Stein et al., 1993; Stirling et al., 1998; Tudhope et al., 2001). f) Marine Isotope Stages (following EPICA community members, 2006).

deposited between ~135 and ~120 ka. S2 and S3 were deposited between ~120 and ~90 ka and between ~90 and ~75 ka, respectively.

3) During the deposition of sequence S1 (~135–120 ka), Lake Samra rose from under 380 m below MSL to ~320 m below MSL. During the deposition of sequence S2 (~118–116 ka) the lake first declined to 340–350 m below MSL and then rose to ~310–320 m below MSL at ~115 to ~90 ka. Following the S3 sequence the lake dropped to levels lower than ~380 m below MSL, before the rise of Lake Lisan at ~75 ka.
4) Significant lake-level declines occurred during global sea-level rises (at ~135 ka, ~118 ka and ~80 ka), while higher lake-stands occurred during cold events in the Northern Hemisphere (e.g., MIS 5b and 5d). Similar patterns were recorded for the last glacial Lake Lisan (highstand) and the Holocene Dead Sea (lowstand). This calls for a persistent linkage between climatic conditions in the Northern Hemisphere and those in the east Mediterranean, which is the main source of rain falling over the DSB drainage area. Cold conditions in the northern hemisphere were recorded by increase wetness in the drainage area and warm (e.g., last interglacial) by arid conditions.
5) During the lowstand intervals of Lake Samra, when Mediterranean rains were more limited, travertines and speleothems were deposited in the southern Arava–Negev deserts. The occurrence of these deposits suggests enhanced activity of a southern source of wetness during the last interglacial period, compared to the current hydrological conditions in the Dead Sea.

Acknowledgments

This study benefited from constructive assistance of numerous people both in the lab and the field. Among all, we would like to thank Eitan Shelef, Adi Torfstein and Boaz Tatarsky for their productive discussions and assistance during fieldwork. Yuval Bartov, Revital Bookman, Efrat Farber, Nissim Hazan and Elisa Kagan are also kindly acknowledged for their discussions and fruitful help. We also thank Anton Vaks and Mira Bar-Matthews for alpha-counting U/Th measurements of several Samra samples and helpful discussions. The field expeditions could not have been accomplished without the assistance and logistic support of the Geological Survey of Israel. The manuscript profited from constructive reviews of Tzvia Schweitzer and Milan Beres. We owe major improvement of this article to the outstanding reviews of Prof. Yehouda Enzel and Dr. Claire Rambeau. The work was supported by a GIF grant (#I-805.221.8/2003 to MS).

Appendixes

All the columnar sections are measured from the exposure base (whether in the Samra or Amora formations) until a prominent triple gypsum sequence of the Lisan Formation that served as a lithological marker for further comparison among the columnar sections. The chronology is based on several U/Th ages measured by Thermal Ionization Mass Spectrometer (TIMS) in the Geological Survey of Israel. The legend for all sites is at Appendix A.

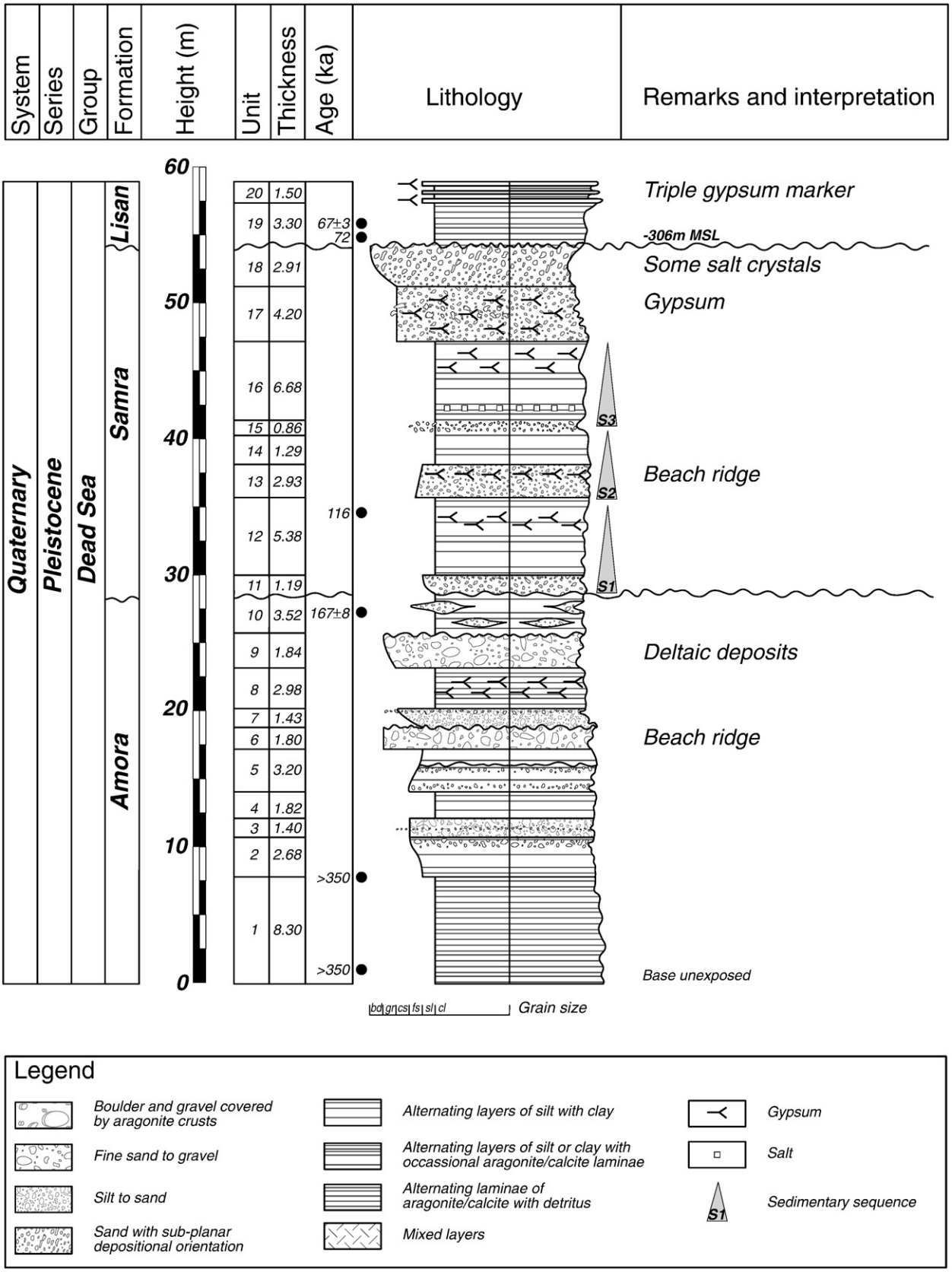

Appendix A. Detail description of the Perazim (PZ7) columnar section. The site is located at coordinates 18450/05580 on the base and 18517/05700 on the top of the columnar section (New Israeli Grid projection).

https://doi.org/10.1016/j.yqres.2009.03.005 Published online by Cambridge University Press

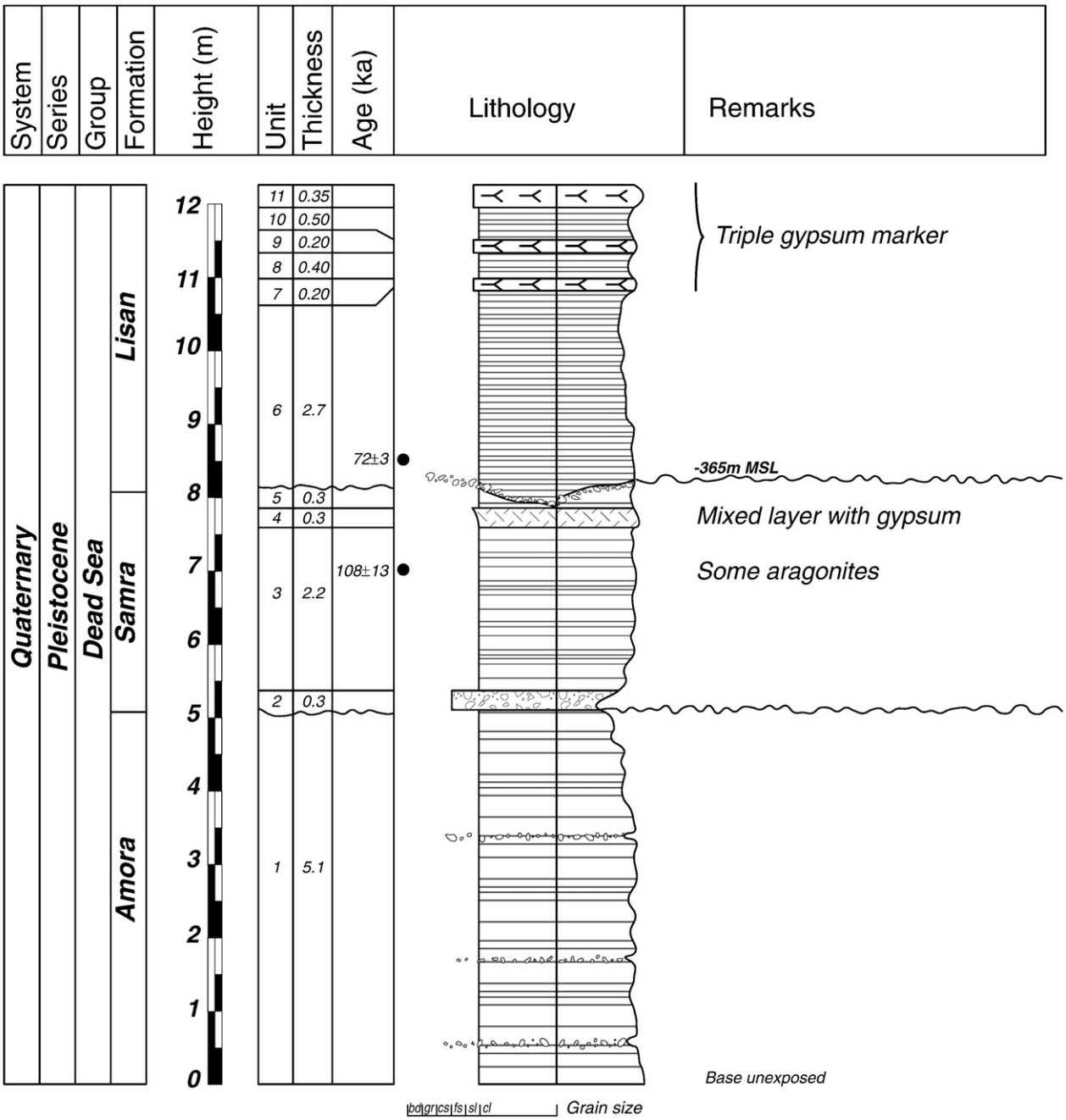

Appendix B. Detail description of the Bet Ha'Arava (BA) columnar section. The site is located at coordinates 19845/13395 (New Israeli Grid projection).

https://doi.org/10.1016/j.yqres.2009.03.005 Published online by Cambridge University Press

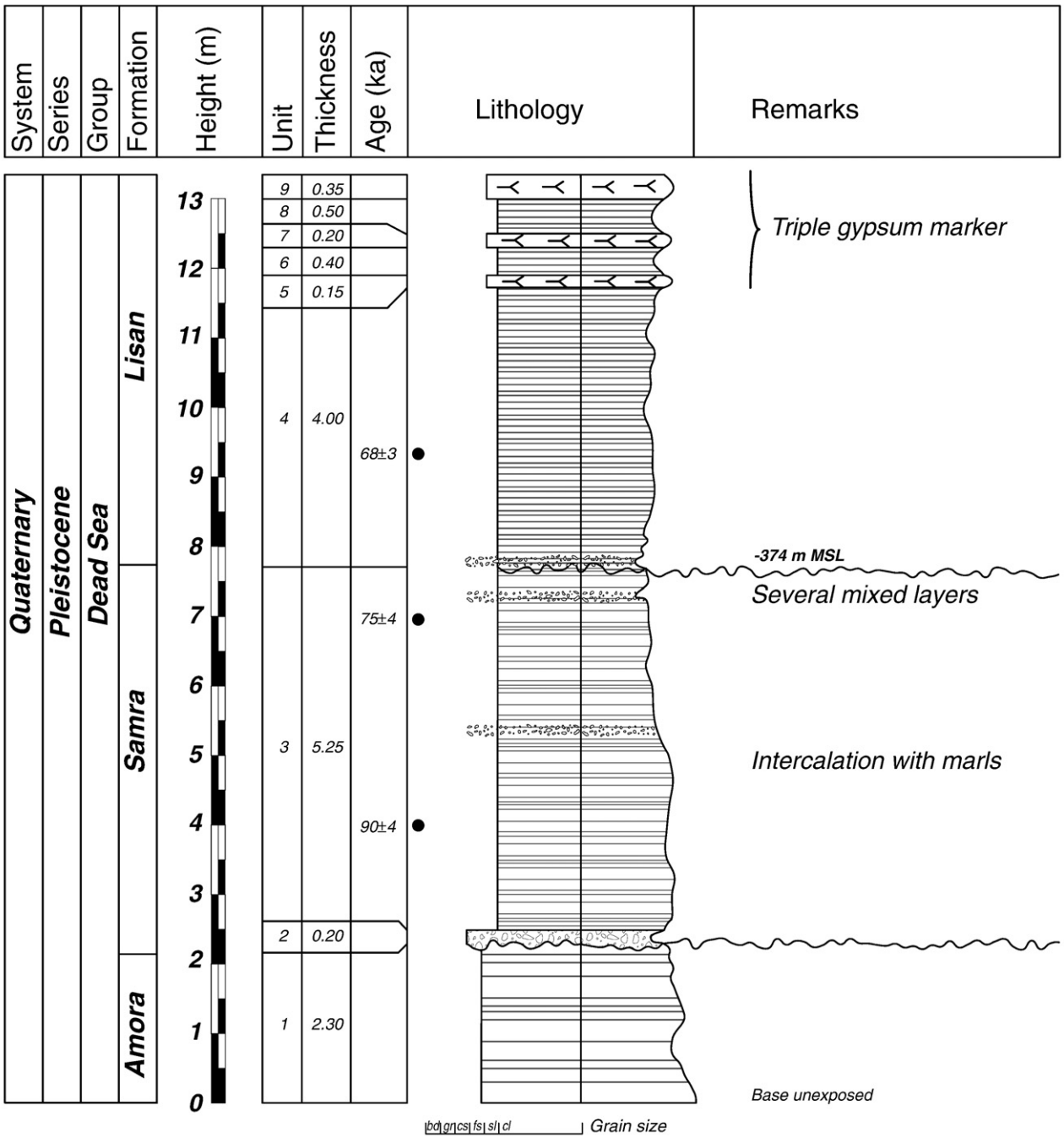

Appendix C. Detail description of the Massada (MZ) columnar section. Coordinates: 18575/07955 (New Israeli Grid projection).

https://doi.org/10.1016/j.yqres.2009.03.005 Published online by Cambridge University Press

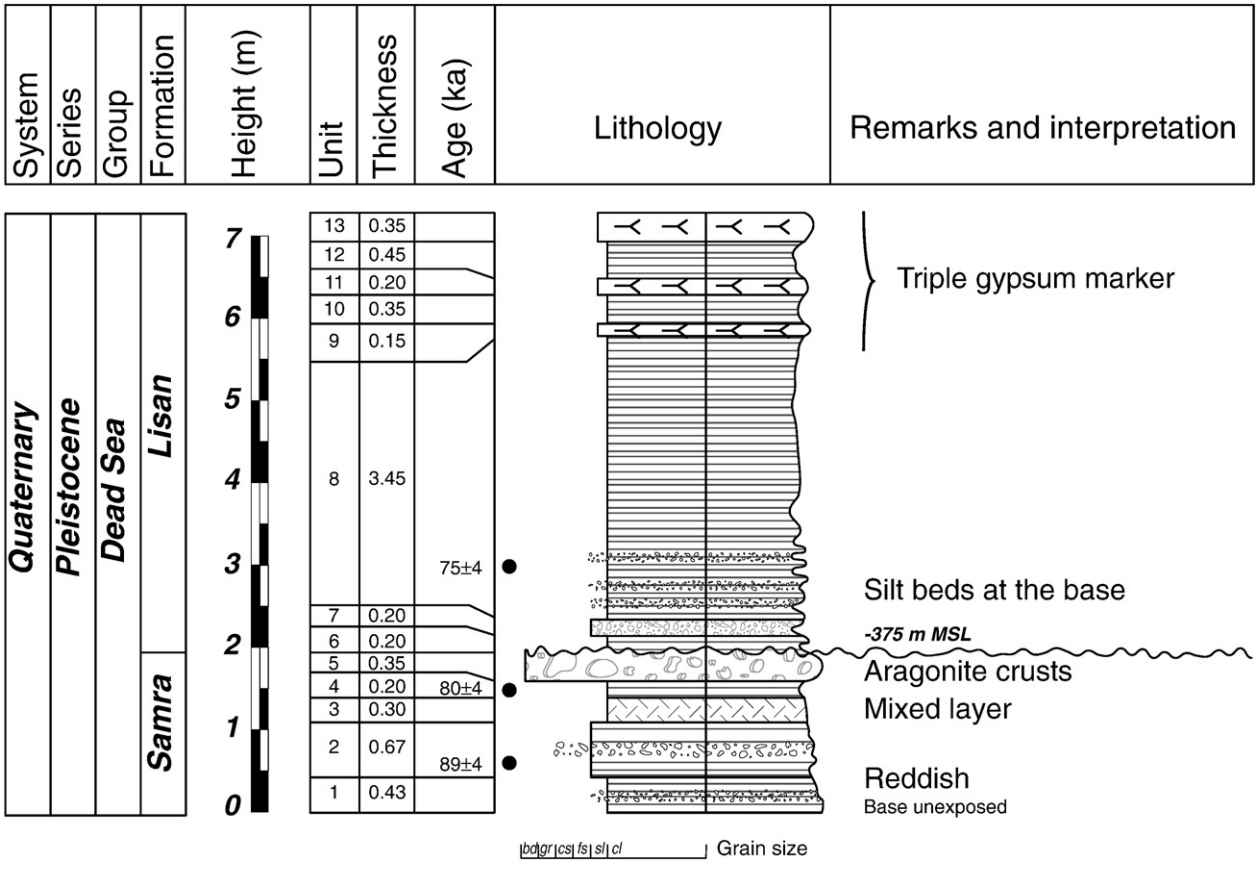

Appendix D. Detail description of the Mishmar (MS) columnar section. Coordinates: 18600/08615 (New Israeli Grid projection).

https://doi.org/10.1016/j.yqres.2009.03.005 Published online by Cambridge University Press

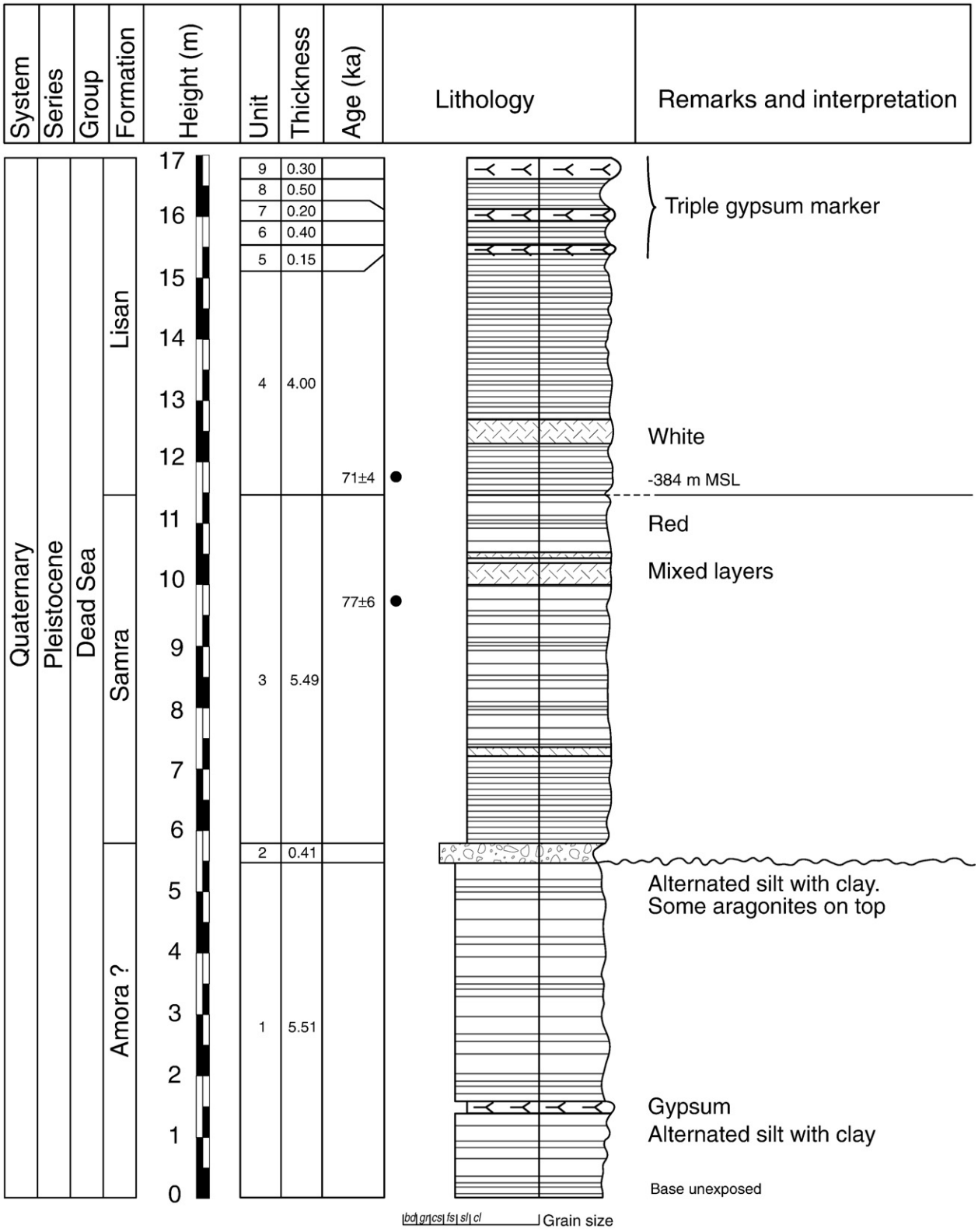

Appendix E. Detail description of the Mor (MR) columnar section. Coordinates: 18570/17425 (New Israeli Grid projection).

https://doi.org/10.1016/j.yqres.2009.03.005 Published online by Cambridge University Press

References

Bar-Matthews, M., Ayalon, A., Gilmour, M., Matthews, A., Hawkesworth, C.J., 2003. Sea-land oxygen isotopic relationships from planktonic foraminifera and speleothems in the Eastern Mediterranean region and their implication for paleorainfall during interglacial intervals. Geochimica et Cosmochimica Acta 67, 3181–3199.

Bartov, Y., Stein, M., Enzel, Y., Agnon, A., Reches, Z., 2002. Lake levels and sequence stratigraphy of Lake Lisan, the Late Pleistocene precursor of the Dead Sea. Quaternary Research 57, 9–21.

Bartov, Y., Goldstein, S.L., Stein, M., Enzel, Y., 2003. Catastrophic arid episodes in the Eastern Mediterranean linked with the North Atlantic Heinrich events. Geology 31 (5), 439–442.

Bartov, Y., Agnon, A., Enzel, Y., Stein, M., 2006. Late Quaternary faulting and subsidence in the central Dead Sea basin. Israel Journal of Earth Sciences 55, 17–31.

Bartov, Y., Enzel, Y., Porat, N., Stein, M., 2007. Evolution of the Late Pleistocene–Holocene Dead Sea basin from sequence statigraphy of fan deltas and lake-level reconstruction. Journal of Sedimentary Research 77, 680–692.

Begin, Z.B., 1975. Paleocurrents in the Plio-Pleistocene Samra Formation (Jericho region, Israel) and their tectonic implication. Sedimentary Geology 14, 191–218.

Begin, Z.B., Ehrlich, A., Nathan, Y., 1974. Lake Lisan the Pleistocene precursor of the Dead Sea. Geological Survey of Israel Bulletin 63, 1–30.

Ben-Avraham, Z., 1997. Geophysical framework of the Dea Sea: structure and tectonics. In: Niemi, T.M., Ben-Avraham, Z., Gat, J.R. (Eds.), The Dead Sea, the Lake and its Setting. Oxford University Press, New York, pp. 22–35.

Ben-Avraham, Z., Schubert, G., 2006. Deep "drop down" basin in the southern Dead Sea. Earth and Planetary Science Letters 251, 254–263.

Bentor, Y.K., Vroman, A., 1960. The geological map of Israel on a 1:100,000 scale; series A, The Negev, sheet 16, Mount Sdom, 2nd ed. .

Bookman (Ken-Tor), R., Enzel, Y., Agnon, A., Stein, M., 2004. Late Holocene lake levels of the Dead Sea. Geological Society of America Bulletin 116 (5/6), 555–571.

Bookman, R., Bartov, Y., Enzel, Y., Stein, M., 2006. Quaternary lake levels in the Dead Sea basin: two centuries of research. In: Enzel, Y., Agnon, A., Stein, M. (Eds.), New Frontiers in Dead Sea Paleoenvironmental Research. Geological Society of America Special Paper, 401, pp. 155–170.

Cutler, K.B., Edwards, R.L., Taylor, F.W., Cheng, J., Adkins, J., Gallup, C.D., Cutler, P.M., Burr, G.S., Bloom, A.L., 2003. Rapid sea-level fall and deep-ocean temperature change since the last interglacial period. Earth and Planetary Science Letters 206, 253–271.

Enmar, L., 1999. The travertines in the Northern and Central Arava: stratigraphy, petrology and geochemistry. Geological Survey of Israel Report 1/99.

Enzel, Y., Bookman (Ken-Tor), R., Sharon, D., Gvirtzman, H., Dayan, U., Ziv, B., Stein, M., 2003. Late Holocene climates of the Near East deduced from Dead Sea level variations and modern regional winter rainfall. Quaternary Research 60, 263–273.

Enzel, Y., Agnon, A., Stein, M., 2006. New frontiers in Dead Sea paleoenvironmental research. Geological Society of America Special Paper 401 253pp.

EPICA community members, 2006. One-to-one coupling of glacial climate variability in Greenland and Antarctica. Nature 444, 195–198.

Fontugne, M., Calvert, S.E., 1992. Late Pleistocene variability of the carbon isotopic composition of organic matter in the eastern Mediterranean: monitor of changes in carbon sources and atmosphere CO^2 concentrations. Paleoceanography 7, 1–20.

Garfunkel, Z., 1981. Internal structure of the Dead Sea Leaky Transform (rift) in relation to plate kinematics. Tectonophysics 80, 81–108.

Hearty, P.J., Hollin, J.T., Neumann, A.C., O'Leary, M.J., McCulloc, M., 2007. Global sea-level fluctuations during the Last Interglaciation (MIS 5e). Quaternary Science Reviews 26, 2090–2112.

Katz, A., Kolodny, Y., Nissenbaum, A., 1977. The geochemical evolution of the Pleistocene Lake Lisan — Dead Sea system. Geochimica et Cosmoquimica Acta 41, 1609–1629.

Kaufman, A., Yechieli, Y., Gardosh, M., 1992. Reevaluation of the Lake-sediment chronology in the Dead Sea Basin, Israel, based on new ^{230}Th/U dates. Quaternary Research 38, 292–304.

Kolodny, Y., Stein, M., Machlus, M., 2005. Sea-rain-lake relation in the Last Glacial East Mediterranean revealed by $\delta^{18}O$–$\delta^{13}C$ in Lake Lisan aragonites. Geochimica Cosmochimica Acta 69, 4045–4060.

Langozky, Y., 1961. Remarks on the petrography and geochemistry of the Lisan Marl Formation. Unpublished MSc thesis, The Hebrew University, Jerusalem, Israel (in Hebrew).

Machlus, M., Enzel, Y., Goldstein, S.L., Marco, S., Stein, M., 2000. Reconstruction low levels of Lake Lisan by correlating fan-delta and lacustrine deposits. Quaternary International 73 (/74), 137–144.

Manspeizer, W., 1985. The Dead Sea rift: impact of climate and tectonism on Pleistocene and Holocene sedimentation. In: Briddle-Kevin, T., Christie-Blick, N. (Eds.), Strike Slip Deformation, Basin Formation and Sedimentation. Society of Economic Paleontologists and Mineralogists Special Publication, 37, pp. 143–158.

Migowski, C., Stein, M., Prasad, S., Negendank, J.F.W., Agnon, A., 2006. Holocene climate variability and cultural evolution in the Near East from the Dead Sea sedimentary record. Quaternary Research 66, 421–431.

Neev, D., Emery, K.O., 1967. The Dead Sea, depositional processes and environments of evaporites. Geological Survey of Israel Bulletin 41, 1–147.

Picard, L., 1943. Structure and evolution of Palestine (with comparative notes on neighboring countries). Geological Department Bulletin, The Hebrew University, Jerusalem 4, 34 pp.

Posamentier, H.W., Allen, G.P., James, D.P., Tesson, M., 1992. Forced regression in a sequence stratigraphic framework: concepts, examples and exploration significance. Bulletin of American Association of Petroleum Geologists 76, 1687–1709.

Rot, I., 1969. The geology of Wadi-el-Qelt area. Unpublished MSc. thesis, The Hebrew University, Jerusalem, Israel (in Hebrew, English summary).

Schramm, A., Stein, M., Goldstein, S.L., 2000. Calibration of ^{14}C time scale to>40 ka by ^{234}U–^{230}Th dating of Lake Lisan sediments (last glacial Dead Sea). Earth and Planetary Science Letters 175, 27–40.

Sneh, A., 1982. Quaternary of the Northwestern 'Arava. Israel. Israel Journal of Earth Sciences 31, 9–16.

Stein, M., 2001. The sedimentary and geochemical record of Neogene-Quaternary water bodies in the Dead Sea Basin — inferences for the regional paleoclimatic history. Journal of Paleolimnology 26, 274–282.

Stein, M., Goldstein, S.L., 2006. U-Th and radiocarbon chronologies of late Quaternary lacustrine records of the Dead Sea basin: methods and applications. In: Enzel, Y., Agnon, A., Stein, M. (Eds.), New Frontiers in Dead Sea Paleoenvironmental Research. Geological Society of America Special Paper, 401, pp. 141–154.

Stein, M., Wasserburg, G.J., Aharon, P., Chen, J.H., Zhu, Z.R., Bloom, A., Chappell, J., 1993. TIMS U-series dating and stable isotopes of the last interglacial event in Papua New Guinea. Geochimica et Cosmochimica Acta 57, 2541–2554.

Stein, M., Starinsky, A., Katz, A., Goldstein, S.L., Machlus, M., Schramm, A., 1997. Strontium isotopic, chemical, and sedimentological evidence for the evolution of Lake Lisan and the Dead Sea. Geochimica et Cosmoquimica Acta 61, 3975–3992.

Stirling, C.H., Esat, T.M., Lambeck, K., McCulloch, M.T., 1998. Timing and duration of the Last Interglacial: evidence for a restricted interval of widespread coral reef growth. Earth and Planetary Science Letters 160, 745–762.

Torfstein, A., 2008. Brine-freshwater interplay and effects on the evolution of saline lakes: the Dead Sea Rift terminal lakes. Geological Survey of Israel, Report GSI/20/2008.

Torfstein, A., Gavrieli, I., Katz, A., Kolodny, Y., Stein, M., 2008. Gypsum as a monitor of the paleo-limnological–hydrological conditions in Lake Lisan and the Dead Sea. Geochimica et Cosmochimica Acta 72, 2491–2509.

Tudhope, A.W., Chilcott, C.P., McCulloch, M.T., Cook, E.R., Chappell, J., Ellam, R.M., Lea, D. W., Lough, J.M., Shimmield, G.B., 2001. Variability in the El Niño-Southern Oscillation though a glacial–interglacial cycle. Science 291, 1511–1517.

Vaks, A., Bar-Matthews, M., Ayalon, A., Matthews, A., Frumkin, A., Dayan, U., Halicz, L., Almogi-Labin, A., Schilman, B., 2006. Paleoclimate and location of the border between Mediterranean climate region and the Saharo-Arabian Desert as revealed by speleothems from the northern Negev Desert. Israel. Earth Planetary Science Letters 249, 384–399.

Waldmann, N., 2002. The Geology of the Samra Formation in the Dead Sea Basin. Unpublished MSc thesis, The Hebrew University, Jerusalem, Israel (in English, Hebrew summary).

Waldmann, N., Starinsky, A., Stein, M., 2007. Primary carbonates and Ca-Chloride brines as monitors of paleo-hydrological regime in the Dead Sea basin. Quaternary Science Reviews 26, 2219–2228.

Weinberger, R., Yechieli, Y., Sneh, A., 2000. The Samra Formation in the Amiaz Plain: stratigraphic correlations of Pre-Lisan lake sediments in the Dead Sea rift. Geological Survey of Israel, Current Research 12, 231–234.

Zak, I., 1967. The geology of Mount Sedom. Unpublished PhD thesis, The Hebrew University, Jerusalem, Israel (in Hebrew, English summary).

https://doi.org/10.1016/j.yqres.2009.03.005 Published online by Cambridge University Press